UPPER-CONVECTED MAXWELL FLUID ANALYSIS OVER A HORIZONTAL WEDGE USING CATTANEO-CHRISTOV HEAT FLUX MODEL

by

Muhammad Solleh ASMADI[a], Ruhaila Md. KASMANI[b*], Zailan SIRI[a], and Sivanandam SIVASANKARAN[c]

[a] Institute of Mathematical Sciences, Faculty of Science,
University of Malaya, Kuala Lumpur, Malaysia
[b] Mathematics Division, Center For Foundation Studies in Science,
University of Malaya, Kuala Lumpur, Malaysia
[c] Department of Mathematics, King Abdulaziz University,
Jeddah, Saudi Arabia

Original scientific paper
https://doi.org/10.2298/TSCI190504270A

Boundary-layer flow of upper-convected Maxwell fluid over a wedge with suction and heat generation/absorption is presented in this paper by considering the Cattaneo-Christov heat flux model. The governed equations are transformed into a set of the ODE using similarity transformations. A third-order finite difference method for the ODE is used to find the local similarity solutions of the problems. The effects of the wedge angle parameter, viscoelastic fluid parameter, thermal relaxation time parameter, and heat generation/absorption parameter are presented in this study.

Key words: *upper-convected Maxwell fluid, Cattaneo-Christov heat flux model, finite difference method, heat generation/absorption, suction, horizontal wedge,*

Introduction

The non-Newtonian fluid dynamics is a continuously expanding field in the multidisciplinary area and in scientific industries due to its application in our daily lives such as human saliva, mustard sauce and toothpaste. The power-law model [1] can be used to describe these fluid behaviors. This model, however, did not explain the characteristics of viscoelastic of the fluid, which is a common trait for most of the fluid. To overcome this shortcoming, upper-convected Maxwell (UCM) fluid model is used since it is a viscoelastic fluid model that includes fluid relaxation time. There are many studies conducted around UCM fluid model which are done by [2-5].

Heat transfer occurs in many phenomena in industrial applications such as water heater, nuclear cooling and heat dissipation in mobile phones. The Fourier law of heat conduction had been used for a long time to describe the heat transfer in a material. The disadvantages of the law are the medium under consideration will be affected instantly if there is any initial disturbance present due to the parabolic energy equation of the law. To overcome this, Cattaneo [6]

* Corresponding author, e-mail: ruhaila@um.edu.my

modified the law by including a relaxation time for heat flux since he thought the law is unable to describe the heat flow in much of the real fluid.

The modification done by Cattaneo was refined by Christov [7] by considering the Oldroyd upper convective derivatives so the model is now frame-indifferent and time-invariant. The investigation of the heat transfer in a fluid governed by Cattaneo-Christov heat flux model is expanding. Some of the work done are shown in [8-11].

Followed by the previous study mentioned previously, there are certain gaps within the scope of the study. The present study is conducted to fill in those gaps which are about the heat transfer of Cattaneo-Christov heat flux model over a horizontal wedge in the presence of suction and heat generation/absorption. The governed PDE are transformed into a set of ODE by using some similarity transformation. The resulting equations are computed numerically using a variation of third-order finite difference method (FDM) published by Pandey [12] and the standardized second-order FDM as outlined in Burden and Faires [13]. The dimensionless parameters involved are investigated further by varying the value correspondingly.

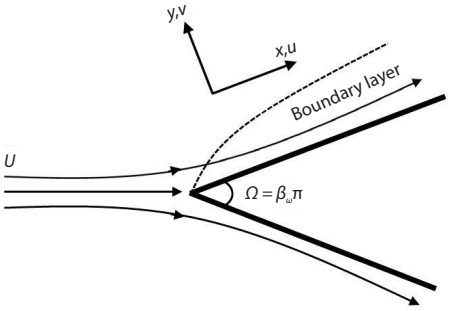

Figure 1. Geometry representation of the fluid

Mathematical formulations

The 2-D laminar flow of UCM fluid over a horizontal wedge with $\Omega = \beta_w \pi$ is the wedge angle, is considered as shown in fig. 1. The parameter β_w is the Hartree pressure gradient. An assumption is made by assumed the plate has a constant temperature T_w, and the ambient fluid temperature is T_∞. The governed equation for the steady incompressible laminar flow of UCM fluid over a horizontal wedge with no-slip velocity, heat transfer, constant suction, and heat generation/absorption is expressed:

$$\frac{\partial u}{\partial x} + \frac{\partial v}{\partial y} = 0 \tag{1}$$

$$u\frac{\partial u}{\partial x} + v\frac{\partial u}{\partial y} + \lambda_1\left(u^2\frac{\partial^2 u}{\partial x^2} + v^2\frac{\partial^2 u}{\partial y^2} + 2uv\frac{\partial^2 u}{\partial x \partial y}\right) = \nu\frac{\partial^2 u}{\partial y^2} + U\frac{\partial U}{\partial x} + \lambda_1 U^2\frac{\partial^2 U}{\partial x^2} \tag{2}$$

$$\rho C_p\left(u\frac{\partial T}{\partial x} + v\frac{\partial T}{\partial y}\right) = -\nabla\cdot\mathbf{q} + \mu\left(\frac{\partial u}{\partial y}\right)^2 + Q(T - T_\infty) \tag{3}$$

where x, y are the co-ordinates along and normal to the heated plate, respectively, u, v – the velocity components along the x- and y-axis, respectively, λ_1 is the relaxation time of the Maxwell fluid, ν – the kinematic viscosity of the fluid, ρ – the fluid density, C_p – the specific heat capacity of the fluid, T – the local fluid temperature, Q – the heat generation/absorption coefficient, and $\mathbf{q}$ – the heat flux proposed by Cattaneo [6] and Christov [7] which satisfies the following:

$$\mathbf{q} + \lambda_2\left[\frac{\partial \mathbf{q}}{\partial t} + \vec{\mathrm{V}}\cdot\nabla\mathbf{q} - \mathbf{q}\cdot\nabla\vec{\mathrm{V}} + (\nabla\cdot\vec{\mathrm{V}})\mathbf{q}\right] = -k\nabla T \tag{4}$$

where $\vec{\mathrm{V}}$ is the velocity vector, λ_2 – the relaxation time for heat flux, and k – the thermal conductivity of the fluid. For steady incompressible fluid, $(\nabla\cdot\vec{\mathrm{V}})\mathbf{q} = 0$).

By eliminating **q** from eqs. (3) and (4), we obtain the following equation (see Christov [7] and Han *et al*. [14] for details):

$$u\frac{\partial T}{\partial x}+v\frac{\partial T}{\partial y}+\lambda_2\left[u^2\frac{\partial^2 T}{\partial x^2}+v^2\frac{\partial^2 T}{\partial y^2}+2uv\frac{\partial^2 T}{\partial x\partial y}+\left(u\frac{\partial u}{\partial x}+v\frac{\partial u}{\partial y}\right)\frac{\partial T}{\partial x}+\right.$$
$$\left.+\left(u\frac{\partial v}{\partial x}+v\frac{\partial v}{\partial y}\right)\frac{\partial T}{\partial y}\right]=\alpha\frac{\partial^2 T}{\partial y^2}+\mu\left(\frac{\partial u}{\partial y}\right)^2+Q(T-T_\infty) \tag{5}$$

For the purpose of study of this paper, the viscoelastic dissipation term $\mu(\partial u/\partial y)^2$ on eq. (5) can be neglected since for the term to be significant, the free stream velocity, U, of the fluid must approach the speed of sound for a lower Prandtl number, such as gases [15]. Another reason of the omission of the viscoelastic dissipation term is because the term only have a significant effect when the fluid becomes elastic ($\beta > 1$), where β is the local Deborah number for the velocity profile, and the scope of this paper is for purely viscous fluid ($\beta < 1$). Thus, $\mu(\partial u/\partial y)^2 = 0$.

The boundary conditions are:

$$\begin{aligned} u=0,\ v=\tilde{v}_0,\ T=T_w\ \text{ at }\ y=0 \\ u\to U,\ T\to T_\infty\ \text{ as }\ y\to\infty \end{aligned} \tag{6}$$

where $\tilde{v}_0$ is suction and $U = ax^m$ with a is a constant and m is the wedge angle parameter and a function of β_w, such that $m = (\beta_w/2 - \beta_w)$. The following transformation is used:

$$\eta=y\sqrt{\frac{(m+1)U}{2\nu x}},\quad \psi=f(\eta)\sqrt{\frac{2U\nu x}{m+1}},\quad \theta(\eta)=\frac{T-T_\infty}{Tw-T_\infty} \tag{7}$$

By eq. (7), eq. (1) is automatically satisfied and eq. (2) together with eq. (5) are then transformed into the set of ODE:

$$f'''+\frac{2m}{m+1}[1-(f')^2]+ff''+$$
$$+\beta\left[2m\frac{m-1}{m+1}[1-(f')^3]-\frac{m-1}{2}\eta(f')^2f''-\frac{m+1}{2}f^2f'''+(3m-1)ff'f''\right]=0 \tag{8}$$

$$\theta''+\mathrm{Pr}\,f\theta'+\frac{2}{m+1}\mathrm{Pr}\,\delta\theta-\mathrm{Pr}\,\gamma\left[\frac{m+1}{2}f^2\theta''-\frac{6}{m+1}\eta(f')^2\theta'+ff'\theta'\right]=0 \tag{9}$$

and the boundary conditions on eq. (7) are reduced into the following dimensionless boundary condition:

$$\begin{aligned} f=\frac{2}{m+1}s,\ f'=0,\ \theta=1\ \text{ at }\ \eta=0 \\ f'\to 1,\ \theta\to 0\ \ as\ \ \eta\to\infty \end{aligned} \tag{10}$$

where $\beta = \lambda_1 U/(2x)$ is the viscoelastic fluid parameter, $\gamma = \lambda_2 U/(2x)$ – the dimensionless thermal relaxation time, $\mathrm{Pr} = \nu/\alpha$ – the Prandtl number, $\delta = Q/(ab^2)$ – the heat generation/absorption parameter, and $s = -v_0[(m + 1)/(2U\nu)]^{1/2}$ – the suction parameter where $v_0 = \tilde{v}_0 x^{1/2}$. Since the value of β and γ contains the function of x, the similarity solutions of f and θ do not exist. So the availability of the local similarity solutions is used as explained and argued in detail by Hashim and Khan [16], and the solution found can be used to see the effect of parameters to the fluid behavior above the wall. By the aforementioned argument, β and γ are now becoming local Deborah number on the velocity profile f' and temperature distribution θ, respectively.

The expression for local skin-friction coefficient C_f and local Nusselt number:

$$C_f(\mathrm{Re}_x)^{1/2} = \sqrt{\frac{m+1}{2}} f''(0) \tag{11}$$

$$\mathrm{Nu}(\mathrm{Re}_x)^{-1/2} = -\sqrt{\frac{m+1}{2}}\, \theta'(0) \tag{12}$$

where $\mathrm{Re}_x = Ux/\nu$ is the local Reynolds number.

Method of solution

To solve the non-linear boundary value problem eq. (8), a method that was proposed by Pandey [12] is used. For eq. (9), the method of standard second-order finite difference method is used which outlined by Burden and Faires [13].

For eq. (8), N finite numbers of nodal points of domain $[0, a_1]$ are defined where a_1 is a finite value so it approximates $\eta \to \infty$, so that $0 = \eta_0 < \eta_1 < ... < \eta_N = a_1$, with uniform step length, h, such that $\eta_i = ih$, $i = 0, 1,..., N$. Suppose the theoretical solution of eq. (8) is $F(\eta)$ at nodal point η_i, $i = 1, 2,..., N$. The numerical approximation of $f(\eta)$ at node η_i are denoted as f_i, and the following source function as F_i:

$$F_i = \frac{-\frac{2m}{m+1}[1-(f_i')^2] - f_i f_i'' - \beta\left\{2m\frac{m-1}{m+1}[1-(f_i')^3] - \frac{m-1}{2}\eta_i (f')^2 f_i'' + (3m-1) f_i f_i' f_i''\right\}}{1-\frac{m+1}{2}\beta f_i^2} \tag{13}$$

at node η_i. Thus the boundary value problem (8) and the boundary condition (10) can be written:

$$f_i''' = F_i \quad \text{at} \quad \eta = \eta_i,\ 0 < \eta_i < a_1 \tag{14}$$

$$f_0 = \frac{2}{m+1} s,\ f_0' = 0,\ f_N' = 1 \tag{15}$$

The rest of the algorithm are followed as stated by [12].

Equation (9) is solved by dividing the domain $[0, a_1]$ where a_1 is a finite value so it approximates $\eta \to \infty$ into $(N + 1)$ subintervals, where the endpoints are at $\eta_i = ih$, for $i = 0, 1, 2,..., N + 1$ and $h = a_1/N$. Suppose the theoretical solution of eq. (9) is $\Theta(\eta)$ at points η_i, $i = 1, 2,..., N + 1$. By considering the central divided difference formula of second-order accuracy, eq. (9) can be written:

$$\frac{-\theta_{i+1} - 2\theta_i + \theta_{i-1}}{h^2} = \Theta_i = 0 \tag{16}$$

where

$$\Theta_i = \frac{-\mathrm{Pr}\, f_i \theta_i' + \frac{2}{m+1}\mathrm{Pr}\,\delta\theta_i - \mathrm{Pr}\,\gamma\left[-\frac{6}{m+1}\eta_i (f_i')^2 \theta_i' + f_i f_i' \theta_i'\right]}{1-\frac{m+1}{2}\mathrm{Pr}\,\gamma f_i^2} \tag{17}$$

with β subject to the following boundary condition:

$$\theta_0 = 1,\quad \theta_{N+1} = 0 \tag{18}$$

The value of f and f' are taken from the final result found when solving eq. (14). The work are continued by following the algorithm as stated in [14].

Results and discussions

All computations were done with tolerance level ε of 10^{-5} and the value of suction parameter s is fixed to be 0.1, because the main study of this paper is to see the difference of the velocity and temperature profile for different values of parameters while the fluid experiencing suction. Table 1 shows the comparison of the value of $f''(0)$ for different values of m obtained from the previous study with present works with $\beta = \gamma = s = \delta = 0$ and Pr = 1. It is shown that the results produced are in good agreement with other works.

Table 1. Comparison of the value of $f''(0)$ from previous study with present works

m	[17]	[18]	[19]	Present
0.0000	0.469600	0.469600	–	0.469443
0.0141	0.504614	–	–	0.506152
0.0909	0.654979	0.655000	0.65498	0.655053
0.2000	0.802125	0.802100	0.80213	0.802897
0.3333	0.927653	0.927700	0.92765	0.927739

Table 2. The physical properties for selected fluid

Fluid	Pr	T_∞ [°C]	v [m^{2}s^{-1}]
Gaseous ammonia	1.5-2	25	$1.45 \cdot 10^{-5}$

The dimensional form for several different types of system is presented. Table 2 shows the physical properties of fluid used as an example of several systems. Figure 2 presented the heat map of gaseous ammonia with wedge angle parameter $m = 0$, while fig. 3 presented the heat map of gaseous ammonia with wedge angle parameter $m = 0.2$, both at a constant T_∞, T_w, U, β, γ, and δ. The value $m = 0$ corresponds to a flat horizontal plate. Based on figs. 2 and 3, it can be seen that the thermal boundary-layer for $m = 0$ is thicker than $m = 0.2$. This means the heat dissipation in a fluid past a horizontal wedge is more efficient than the heat dissipation in a fluid past a horizontal plate.

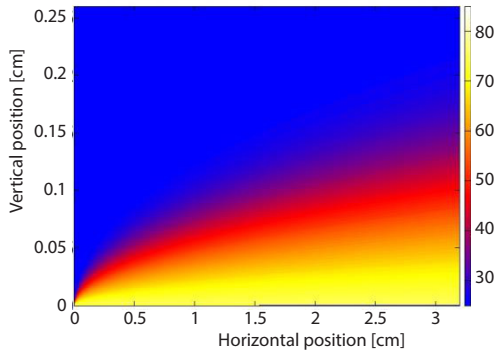

Figure 2. The heat map of gaseous ammonia with $m = 0$ at $T_\infty = 25$ °C with $T_w = 75$ °C, $U = 1$ m/s, and $\beta = \gamma = \delta = 0.2$

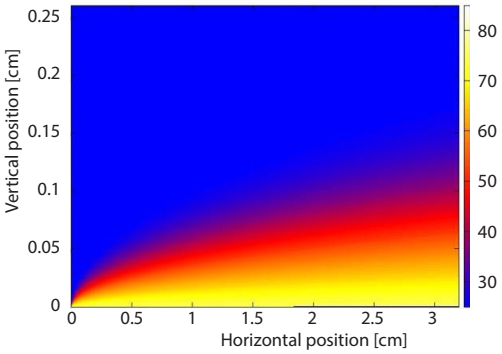

Figure 3. The heat map of gaseous ammonia with $m = 0.2$ at $T_\infty = 25$ °C with $T_w = 75$ °C, $U = 1$ m/s, and $\beta = \gamma = \delta = 0.2$

Figure 4 presented the heat map of gaseous ammonia with heat generation/absorption parameter $\delta = -0.2$, while fig. 5 presented the heat map of gaseous ammonia with heat generation/absorption parameter $\delta = 0.2$, both at a constant T_∞, T_w, U, β, and γ. It is shown from

figs. 4 and 5 that the thermal boundary-layer for $\delta = -0.2$ is much thinner than the thermal boundary-layer for $\delta = 0.2$. This means that as δ increases, the thermal boundary-layer thickens. For $\delta < 0$, it denotes the heat absorption and $\delta > 0$ indicates the heat generation. Thus, based on figs. 4 and 5, it can be said that the presence of heat absorption helps the heat to dissipate quicker from the system, while the presence of heat generation retards the heat transfer. As a conclusion, as δ increases, the efficiency of heat dissipation from the wall in the fluid-flow decreases.

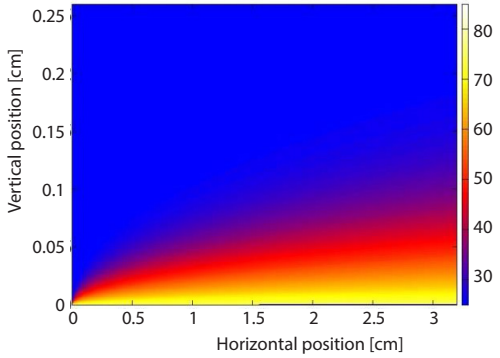

Figure 4. The heat map of gaseous ammonia with with $\delta = -0.2$, at $T_\infty = 25$ °C with $T_w = 75$ °C, $U = 1$ m/s, $m = 0.0141$ and $\beta = \gamma = 0.2$

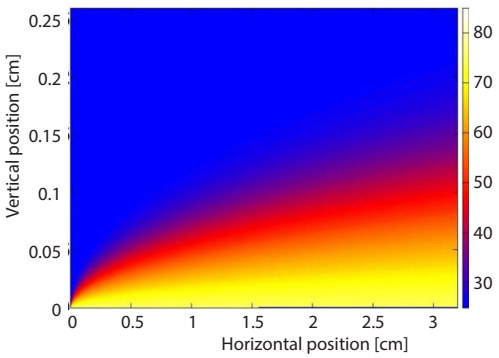

Figure 5. The heat map of gaseous ammonia with with $\delta = 0.2$, at $T_\infty = 25$ °C with $T_w = 75$ °C, $U = 1$ m/s, $m = 0.0141$ and $\beta = \gamma = 0.2$

The effect of the wedge angle parameter, m, on the velocity profile and temperature profile is presented in fig. 6. As wedge angle parameter, m, increases, the velocity profile f' increases while the temperature profile θ decreases. The value $m = 0$ corresponds to a horizontal plate (0°) and $m = 1$ illustrates the stagnation point of a vertical plate (180°). This means as the wedge becomes steeper, the thickness of momentum and thermal boundary-layer decreases. This result corresponds to the results shown in figs. 2 and 3 where as m increases, the heat transfer rate of the fluid increases, thus produced a thinner thermal boundary-layer. In fig. 7, the effect of the local Deborah number, β, on the velocity and temperature profile are shown. Based on fig. 7, the velocity profile decreases slightly while β increases slightly. On the other hand, the temperature profile increases for the increasing value of β. The local Deborah number for fluid momentum is defined as the ratio of fluid relaxation time to its deformation time. As β increases, the relaxation time of the fluid increases. As a result, it causes the thickness of momentum

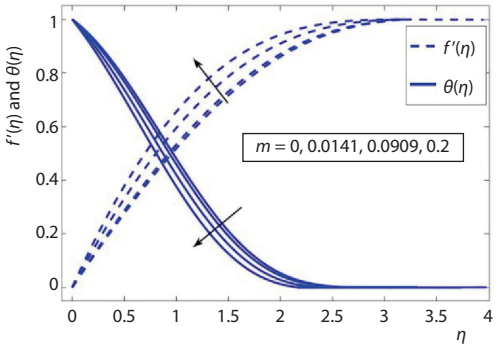

Figure 6. The velocity profile and temperature profile for different values of m with $\beta = \gamma = \delta = 0.2$, and Pr = 2

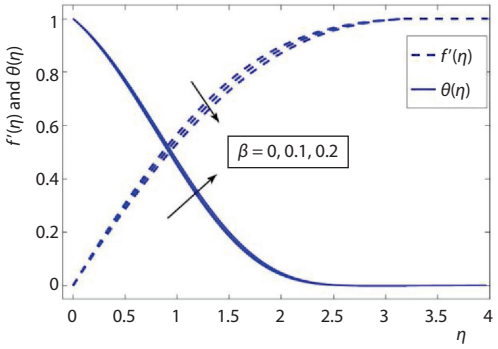

Figure 7. The velocity profile and temperature profile for different values of β with $m = 0.0141$, $\gamma = \delta = 0.2$, and Pr = 2

and the thermal boundary-layer increases. Based on fig. 7, it can be concluded that the changes in the value of β do affect the velocity and temperature profile slightly.

The variation of the fluid temperature distribution, θ, against the different value of the local Deborah number for thermal profile is plotted in fig. 8. In fig. 8, the temperature profile decreases slightly for increasing γ. With the same argument as β, as γ increases, the relaxation time of the heat transfer of the fluid increases and delays the time for the fluid to experience heat conduction. This causes the thermal boundary-layer becomes thinner and results in faster heat dissipation. Since the effect is not significant, it can be concluded that the changes in the value of γ do not affect the thermal boundary-layer in a greater magnitude.

Figure 9 showed the effect of heat generation/absorption parameter δ to the fluid temperature profile θ. In fig. 9, it can be seen that the temperature profile of the fluid increases with the increasing δ. For $\delta < 0$, it denotes the heat absorption and $\delta > 0$ indicates the heat generation. For $\delta > 0$, since it generates more heat, the temperature profile increases as it takes into account the extra heat generated from the fluid. As a contrary, for $\delta < 0$, it absorbs heat energy, thus the temperature profile decreases. This means, as δ increases, the temperature profile increases, causes the thickness of the boundary-layer increases, *i. e.* becomes thicker.

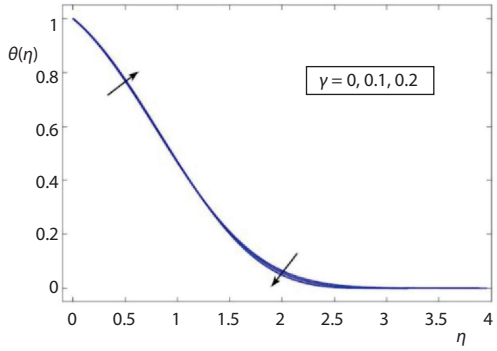

Figure 8. The temperature profile for different values of γ with m = 0.0141, $\beta = \delta$ = 0.2, and Pr = 2

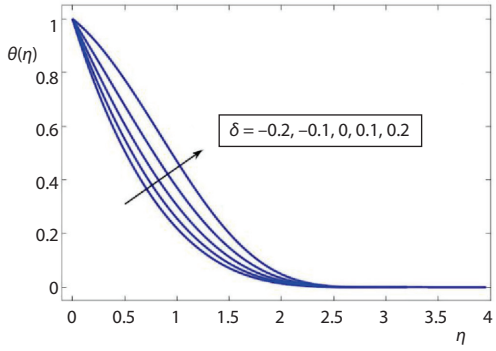

Figure 9. The temperature profile for different values of δ with m = 0.0141, $\beta = \gamma$ = 0.2, and Pr = 2

Figure 10 showed the effect of wedge angle parameter, m, on the local skin friction coefficient, C_f, with different value of β. We notice that the value of C_f increases as m increases and β decreases. For a fixed value of β, a larger wedge angle results in a higher fluid velocity, increases the friction force of the surface of the wedge. Figures 11 and 12 presented the effect of wedge angle parameter m on the local Nusselt number, with different value of γ for fig. 11 and different value of δ on fig. 12. It can be seen from figs. 11 and 12 that the local Nusselt number increases as m increases when γ and δ decreases. Based on fig. 11, for a fixed value of m, as the heat transfer of the fluid follows Cattaneo-Christov heat flux model, the local Nusselt number decreases. From fig. 12, for a fixed wedge angle as the fluid experiences heat absorption, the local

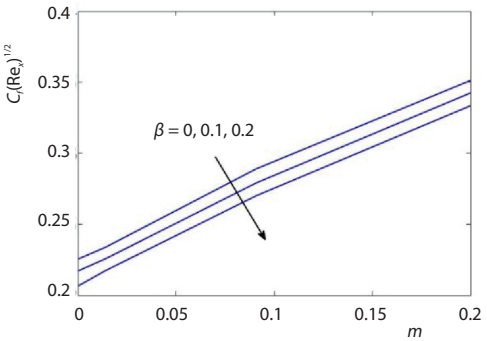

Figure 10. The effect of m to the local skin-friction coefficient for different values of β

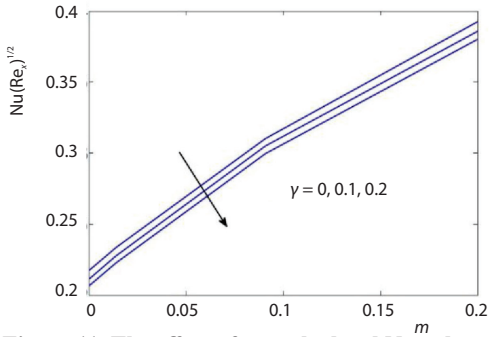

Figure 11. The effect of m to the local Nusselt number for different values of γ

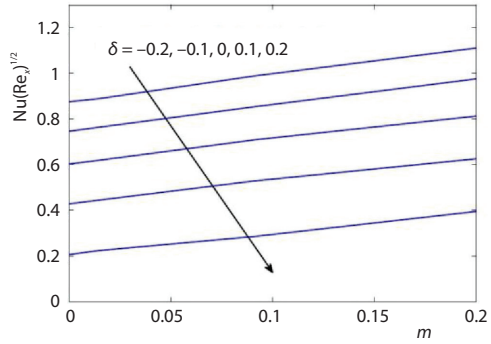

Figure 12. The effect of m to the local Nusselt number for different values of δ

Nusselt number increases, while when the fluid undergoing heat generation, the local Nusselt number decreases.

Conclusions

In this paper, the convective boundary-layer of upper-convected Maxwell fluid over a wedge with suction and heat generation/absorption by considering Cattaneo-Christov heat flux model is investigated. The summary of some important results of the work are listed as follows.

- The increase in wedge angle parameter increases the velocity but decreases the temperature of the fluid.
- Increasing the thermal relaxation time results in some insignificant decrease in the temperature profile of the fluid.
- The temperature profile of the fluid is directly proportional to the heat generation/absorption parameter.

Acknowledgment

The authors would like to acknowledge the Ministry of Higher Education Malaysia and the University of Malaya for the financial support through the Fundamental Research Grant Scheme FP-043-2017A and University of Malaya Research Grant RG397-17AFR.

Nomenclatur

a, b – constants, [–]
a_1 – arbitrary domain boundary, [–]
C_f – local skin-friction coefficient {$= [(m + 1)/2\mathrm{Re}_x]^{1/2} f''(0)$}, [–]
C_p – specific heat capacity, [J°C^{-1}kg^{-1}]
F – momentum source function, [–]
f – dimensionless stream function, [–]
h – uniform stepsize, [–]
k – thermal conductivity, [Wm^{-1}K^{-1}]
m – wedge angle parameter, [–]
N – number of domain division, [–]
Nu – local Nusselt number {$= -[\mathrm{Re}_x(m + 1)/2]^{1/2}\theta'(0)$}, [–]
Pr – Prandtl number ($= \nu/\alpha$), [–]
Q – heat generation/absorption coefficient, [–]
q – heat flux, [Wm^{-2}]
Re_x – local Reynolds number, [–]
s – suction parameter, [–]
T – local fluid temperature, [°C]
T_w – fluid temperature at the surface, [°C]
T_∞ – ambient fluid temperature, [°C]
t – time, [s]
U_w – fluid velocity at the surface, [ms^{-1}]
U – free stream velocity, [ms^{-1}]
u, v – velocity component in x- and y-axis, [ms^{-1}]
v_0 – modified suction, [ms^{-1}]
$\bar{v}_0$ – suction, [ms^{-1}]
x, y – Cartesian co-ordinates, [–]

Greek symbols

α – thermal diffusivity, [m^{2}s^{-1}]
β – local Deborah number for velocity profile, [–]
β_w – Hartree pressure gradient, [–]
γ – local Deborah number for thermal profile, [–]
δ – heat generation parameter, [–]
η – similarity variable, [–]
Θ – thermal source function, [–]
θ – dimensionless temperature, [–]
λ_1 – fluid relaxation time, [s]

λ_2 – heat flux relaxation time, [s]
μ – fluid viscosity, [$kgm^{-1}s^{-1}$]
ν – kinematic viscosity, [m^2s^{-1}]
ρ – fluid density, [kgm^{-3}]
ψ – stream function, [–]
Ω – wedge angle, [°]

Subscripts

w – condition at the surface
∞ – free stream/ambient conditions

Superscript

$'$ – derivatives

Acronyms

FDM – finite difference method
UCM – upper-Convected Maxwell

References

[1] Chhabra, R. P., Non-Newtonian Fluids: An Introduction, in: *Rheology of Complex Fluids*, Springer, New York, USA, 2010, pp. 3-34
[2] Mukhopadhyay, S., Heat Transfer Analysis of the Unsteady Flow of A Maxwell Fluid Over A Stretching Surface in the Presence of A Heat Source/Sink, *Chinese Physics Letters*, *29* (2012), 5, 54703
[3] Hayat, T., *et al*., Mixed Convection Falkner-Skan Flow of A Maxwell Fluid, *ASME-Journal of Heat Transfer*, *134* (2012), 11, 114504
[4] Sadiq, M. A., Hayat, T., Darcy Forchheimer Flow of Magneto Maxwell Liquid Bounded by Convectively Heated Sheet, *Results in Physics*, *6* (2016), C, pp. 884-890
[5] Hayat, T., *et al*., Simultaneous Effects of Heat Generation/Absorption and Thermal Radiation in Magnetohydrodynamics (MHD) Flow of Maxwell Nanofluid Towards A Stretched Surface, *Results In Physics*, *7* (2017), Jan., pp. 562-573
[6] Cattaneo, C., Sulla Conduzione del Calore (On the Heat Conduction – in Italian), *Atti del Seminario Matematico e Fisico dell' Universita di Modena*, *3* (1948), pp. 83-101
[7] Christov, C. I., On Frame Indifferent Formulation of the Maxwell-Cattaneo Model of Finite-Speed Heat Conduction, *Mechanics Research Communications*, *36* (2009), 4, pp. 481-486
[8] Abbasi, F., *et al*., Analytical Study of Cattaneo-Christov Heat Flux Model for A Boundary-Layer Flow of Oldroyd-B Fluid, *Chinese Physics B*, *25* (2015), 1, pp. 1-6
[9] Waqas, M., *et al*., Cattaneo-Christov Heat Flux Model for Flow of Variable Thermal Conductivity Generalized Burgers' Fluid, *Journal of Molecular Fluids*, *220* (2016), Aug., pp. 642-648
[10] Sui, J., *et al*., Boundary-Layer Heat and Mass Transfer with Cattaneo-Christov Double-Diffusion in Upper-Convected Maxwell Nanofluid Past A Stretching Sheet with Slip Velocity, *International Journal of Thermal Sciences*, *104* (2016), June, pp. 461-468
[11] Anjum, A., *et al*., Physical Aspects of Heat Generation/Absorption in the Second Grade Fluid-Flow Due to Riga Plate: Application of Cattaneo-Christov Approach, *Results in Physics*, *9* (2018), June, pp. 955-960
[12] Pandey, P. K., A Numerical Method for the Solution of General Third Order Boundary Value Problem, *Bulletin of the International Mathematical Virtual Institute*, *7* (2017), Jan., pp. 129-138
[13] Burden, R. L., Faires, J. D., *Numerical Analysis*, 9th ed., Cengage Learning, Boston, Mass., USA, 2011
[14] Han, S., *et al*., Coupled Flow and Heat Transfer in Viscoelastic Fluid with Cattaneo-Christov Heat Flux Model, *Applied Mathematics Letters*, *38* (2014), Dec., pp. 87-93
[15] Kays, W. M., Crawford, M. E., *Convective Heat and Mass Transfer*, 3th ed., McGraw-Hill, New Jersey, USA, 1993
[16] Hashim, M. K., Authors Response to the Specious Comment on the Paper, On Cattaneo-Christov Heat Flux Model for Carreau Fluid-flow over A Slendering Sheet, Hashim, Masood Khan, *Results in Physics*, *7* (2017), 310319, *Results in Physics*, *7* (2017), pp. 1799-1800
[17] Yih, K. A., Uniform Suction/Blowing Effect on Forced Convection about A Wedge: Uniform Heat Flux, *Acta Mechanica*, *128* (1998), 3-4, pp. 173-181
[18] Khan, W. A., Pop, I., Boundary-Layer Flow past A Wedge Moving in A Nanofluid, *Mathematical Problems in Engineering*, *2013* (2013), 637285
[19] Kasmani, R., *et al*., Convective Heat Transfer of Nanofluid past A Wedge in the Presence of Heat Generation/Absorption with Suction/Injection, *AIP Conference Proceedings*, *1605* (2014), 1, pp. 506-511

Submitted: May 4, 2019
Revised: May 24, 2019
Accepted: May 27, 2019